Amino Acid Sequences within the α Subunit of Integrin $\alpha_M\beta_2$ (Mac-1) Critical for Specific Recognition of C3bi†

Li Zhang* and Edward F. Plow

Joseph J. Jacobs Center for Thrombosis and Vascular Biology, Department of Molecular Cardiology, The Cleveland Clinic Foundation, 9500 Euclid Avenue, Cleveland, Ohio 44195

Received January 21, 1999; Revised Manuscript Received April 27, 1999

ABSTRACT: Phagocytosis of opsonized particles by neutrophils and monocytes plays a central role in host defense mechanisms against foreign pathogens. This process depends on the interaction between C3bi, a degradation product derived from activation of the complement system, and the $\alpha_M\beta_2$ (CD11b/CD18, Mac-1) receptor, the major integrin on neutrophils. Previous studies had established a central role for the I domain, a stretch of ∼200 amino acids within the α_M subunit in the binding of C3bi, as well as many other $\alpha_M\beta_2$ ligands. The present study was undertaken to establish the molecular basis of C3bi recognition by $\alpha_M\beta_2$. The strategy employed the use of a series of mutant receptors in which short segments of the I domain of α_M were switched to the corresponding segments of α_L, which is structurally very similar but does not bind C3bi. We report three major findings: (1) The C3bi binding pocket is composed of three regions, $P^{147}-R^{152}$, $P^{201}-K^{217}$, and $K^{245}-R^{261}$ of α_M, which surround the cation binding site within the MIDAS motif of the I domain. (2) Within the latter segment, K^{245} plays a critical role in mediating C3bi binding to $\alpha_M\beta_2$. Mutation of K^{245} to Ala significantly reduced C3bi binding but had no effect on binding of another $\alpha_M\beta_2$ I domain ligand, NIF. (3) Blocking of C3bi binding to $\alpha_M\beta_2$ by monoclonal antibodies is achieved through two different mechanisms: direct competition for the ligand binding site or induction of conformational changes. Overall, these studies support the hypothesis that many of the ligands of $\alpha_M\beta_2$ bind to overlapping but not identical sites within the I domain. Although the same short structural segments within the I domain may be involved in binding, different amino acids within these segments may contact different ligands.

Phagocytosis of opsonized particles by neutrophils and monocytes is a major mechanism of host defense against foreign pathogens. This process depends on the interaction between C3bi, a degradation product derived from the activation of the complement system, and the $\alpha_M\beta_2$ (CD11b/CD18, CR3, Mac-1) receptor, the most prominent integrin on neutrophils (*1*). $\alpha_M\beta_2$ is a member of the β_2 integrin subfamily, which includes $\alpha_L\beta_2$ (LFA-1, CD11a/CD18), $\alpha_X\beta_2$ (p150,95, CD11c/CD18), and $\alpha_D\beta_2$. These integrins share a common β subunit of 95 kDa, which is noncovalently linked to distinct but homologous α subunits (*2*, *3*). The physiological functions of $\alpha_M\beta_2$ include roles in adhesion and transmigration of leukocytes through endothelium (*4*), activation of neutrophils and monocytes (*5*), and phagocytosis of foreign materials. In addition, it was shown recently that apoptosis of neutrophils also is controlled by $\alpha_M\beta_2$ (*6*). The importance of the β_2 integrin subfamily in human physiology is underscored by the severe phenotype of individuals with congenital deficiencies of these integrins (*7*). Yet, excessive activation of $\alpha_M\beta_2$ contributes to sustained inflammation, reperfusion injury, and tissue damage (*8*).

$\alpha_M\beta_2$ interacts with a wide variety of protein and nonprotein ligands, including Fg[1] (*9*), ICAM-1 (*10*), C3bi (*11*), and neutrophil inhibitory factor (NIF), a specific $\alpha_M\beta_2$ antagonist isolated from canine hookworms (*12*). The molecular mechanism by which $\alpha_M\beta_2$ can interact with so many structurally unrelated ligands, and yet exhibit high affinity for each, is unknown. Recently, we and others have shown that interactions between C3bi and $\alpha_M\beta_2$ are influenced by both the α and β subunits (*13*−*16*). The I domain, an *inserted* region of ∼200 amino acids in the α_M subunit (α_MI domain), is a major recognition site for C3bi binding to $\alpha_M\beta_2$ (*13*, *14*, *17*). I domains with highly conserved amino acid sequences are also found in several other integrin α subunits as well as in other proteins, such as von Willebrand Factor, and mediate a variety of protein−protein interactions, including ligand binding to integrins (*18*). Regions of the β subunit also may be involved in the recognition of C3bi by $\alpha_M\beta_2$. Specifically, mutations of Asp^{134}, Ser^{136}, or Ser^{138} within a DXSXS sequence conserved within integrin β subunits abrogate the binding of $\alpha_M\beta_2$ to C3bi (*15*, *16*). However, we have recently shown that these residues within the β_2 subunit modulate the recognition of another $\alpha_M\beta_2$ ligand by the I domain of the receptor rather than by directly participating in ligand contact (*19*).

† This work was supported by NIH Grant HL54921 and the American Heart Association.

* Corresponding author. Present address: Department of Vascular Biology, American Red Cross/Holland Laboratory, 15601 Crabbs Branch Way, Rockville, MD 20855.

[1] Abbreviations: EC3bi, C3bi-coated sheep erythrocytes; FACS, fluorescence-activated cell sorting; Fg, Fibrinogen; HBSS, Hank's balanced salt solution; mAb, monoclonal antibody; NIF, neutrophil inhibitory factor; PBS, phosphate-buffered saline.

10.1021/bi990141h CCC: $18.00
Published on Web 06/03/1999

Previously, we have used *homologue-scanning mutagenesis* (*20*) to map the NIF binding site in $\alpha_M\beta_2$ (*21*). This strategy entails switching sequences within the α_MI domain to the homologous sequences within the α_LI domain. A total of 16 segments, corresponding to the outer hydrated surface of α_MI domain, were switched to their counterpart sequences in α_L. Surface expression, heterodimer formation, and appropriate conformational folding were demonstrated for each of the 16 mutants. These mutants were then used to map the NIF binding site to a narrow region composed of three discontinuous segments, $P^{147}-R^{152}$, $P^{201}-K^{217}$, and $D^{248}-R^{261}$, in α_M which lies adjacent to the cation binding site within the I domain. The NIF binding site identified through the loss-of-function mutations was confirmed by a gain-in-function experiment, whereby the I domain of α_X was converted into a NIF binding protein.

Despite its importance in host defense, the C3bi binding pocket within $\alpha_M\beta_2$ remains to be systematically defined. Previous studies (*14*, *22*) have identified a few amino acids that are critical for C3bi binding; however, the residues that impart specific recognition of the ligand to $\alpha_M\beta_2$, as opposed to $\alpha_L\beta_2$, remain unknown. Taking advantage of our existing set of complete I domain homologue-scanning mutants, we have determined the C3bi binding activities of all these 16 mutants and mapped the C3bi binding site to a narrow region within the I domain. In addition, we have studied the mechanism underlying the function of several $\alpha_M\beta_2$ mAbs which block C3bi binding to the receptor. Our data suggest that two different mechanisms are involved in the blocking functions of these mAbs. Moreover, the identified epitopes for these antibodies support our localization of the C3bi binding site in the α_M subunit.

MATERIALS AND METHODS

Materials. Human kidney 293 cells and the expression vector pCIS2M were gifts from Dr. F. J. Castellino (Notre Dame, IN). The cDNAs of CD11b and CD18 were obtained from Dr. B. Karan-Tamir (Amgen, Thousand Oaks, CA), and NIF was provided by Corvas Inc. (San Diego, CA). mAbs 2LPM19c, MHM24, and MHM23 were from Dako (Dako, Carpinteria, CA); TS1/18, TS1/22, OKM1, M1/70, 44a, 904, and LM2/1 were from the ATCC (ATCC, Rockville, MD); 44 was from Sigma (St. Louis, MO); CRIS-3 was from BioSource (Camarillo, CA).

Generation of the Chimeric Receptor. All mutations were created by oligonucleotide-directed mutagenesis using uracil-containing single-stranded M13mp18 DNA (*23*). To switch the I domain between the α_L and α_M, two restriction sites, *Cla*I at position 569 and *Eco*RV site at 1109, were introduced into the α_L cDNA using the following primers: 5′GACCTGGTATTTCTCATCGATGGTTCG3′ and 5′GGCACAAGCAAACAGGATATCACTTCCTTCAACATG3′. An internal *Cla*I site at position 905 was removed using the primer: 5′AGTGGCAACATTGATGCGGCC3′. To replace the α_LI domain with the α_MI domain, the cDNA encoding the α_MI domain was amplified with the following primers: 5′GCAGCAGCCCCAGAAGTT3′ and 5′CGAGCTGATATCTCCTGTCTGAGTACCCTC3′ and then inserted into the full-length α_L using *Cla*I and *Eco*RV restriction sites, generating the chimeric molecule $\alpha_L(I/\alpha_M)$. To express the chimeric heterodimer $\alpha_L(I/\alpha_M)\beta_2$ in 293 cells, the expression vector encoding $\alpha_L(I/\alpha_M)$ (pCIS2m-$\alpha_L(I/\alpha_M)$) was cotransfected with the wild-type β_2 expression vector (pCIS2m-β_2) and the stable cell line was established as described (*23*).

Site-Directed Mutagenesis. The detailed procedures used for homologue-scanning mutagenesis and establishment and characterization of the 16 homologue-scanning mutants have been published (*21*). To obtain mutant cell lines that express equivalent receptor numbers as wild-type $\alpha_M\beta_2$, each mutant cell line was subcloned by limiting dilution. A total of 15 colonies were picked and analyzed for $\alpha_M\beta_2$ expression by FACS analysis. Surface labeling and immunoprecipitation with $\alpha_M\beta_2$ mAbs were performed for all 16 mutant cell lines, confirming heterodimer formation and the appropriate molecular weights for the α_M and β_2 subunits when analyzed on 7% SDS−PAGE. In addition, correct conformations of all 16 mutant receptors were verified by FACS analysis with a panel of $\alpha_M\beta_2$ mAbs, including the conformation-sensitive mAb 24. The procedures for creating single-point mutations within $\alpha_M\beta_2$ have been previously described (*23*). The primers used for K^{245} to D or A mutation within α_M were 5′GGGATCGCCAAAATCTTCTCCATCCGT3′ and 5′GGGATCGCCAAAAGCTTCTCCATCCG3′, respectively. The one for F^{246} to A mutation was 5′CAAGGGATCGCCAGCTTTTTCTCCATC3′.

C3bi Binding to $\alpha_M\beta_2$-Expressing Cells. C3bi binding was performed with slight modification of the method of Bilsland (*24*). Sheep erythrocytes coated with C3bi (EC3bi) were prepared using anti-sheep erythrocyte IgM antibody M1/87 (ATCC, Rockville, MD) and human C5-deficient serum (Sigma, St. Louis, MO). Briefly, 7×10^8 sheep erythrocytes (Colorado Serum Co., Denver, CO) were washed twice in HBSS, containing 5 mM HEPES and 1 mM Mg^{2+}, and coated with IgM as described (*24*). The coated erythrocytes were surface-labeled with biotin using 1 mg of sulfosuccinimidyl 6-(biotinamido)hexanoate (Pierce, Rockford, IL) at 37 °C for 20 min. The biotinylated cells were resuspended in 0.9 mL of HBSS with 5 mM HEPES, 1 mM Ca^{2+}, and 1 mM Mg^{2+}, mixed with 100 μL of C5-deficient serum, and incubated at 37 °C for 60 min. After washing twice, the resulting EC3bi were resuspended in 2 mL of the above solution.

To perform the EC3bi binding assays, a total of 2×10^5 $\alpha_M\beta_2$-expressing cells were seeded onto polylysine (50 μg/mL)-coated 24-well nontissue culture polystyrene plates (Becton Dickinson, Franklin Lakes, NJ) for 15 min at 37 °C, followed by addition of 2×10^7 EC3bi. After 60 min at 37 °C, unbound EC3bi were removed by washing with PBS. Bound EC3bi were fixed with 2% paraformaldehyde overnight, and excess paraformaldehyde was neutralized with 1% BSA at 37 °C for 2 h. Bound EC3bi were quantitated by addition of 300 μL of avidin−alkaline phosphatase conjugate (1:2000 dilution) (Zymed Laboratory, San Francisco, CA). After 90 min at 37 °C, the plates were washed three times with PBS, and 250 μL of 3 mg/mL *p*-nitrophenyl phosphate was added. After a 5-min incubation at 37 °C, the absorbance at 405 nm was determined.

FACS Analysis. For FACS analyses, 10^6 cells in HBSS containing 1 mM Mg^{2+} were incubated with 5 μg of mAb for 30 min at 4 °C. A subtype-matched mouse IgG served as a control. After three washes with PBS, cells were mixed with FITC-goat anti-mouse IgG(H+L) $F(ab')_2$ fragment (1:20 dilution) (Zymed Laboratory), kept at 4 °C for another

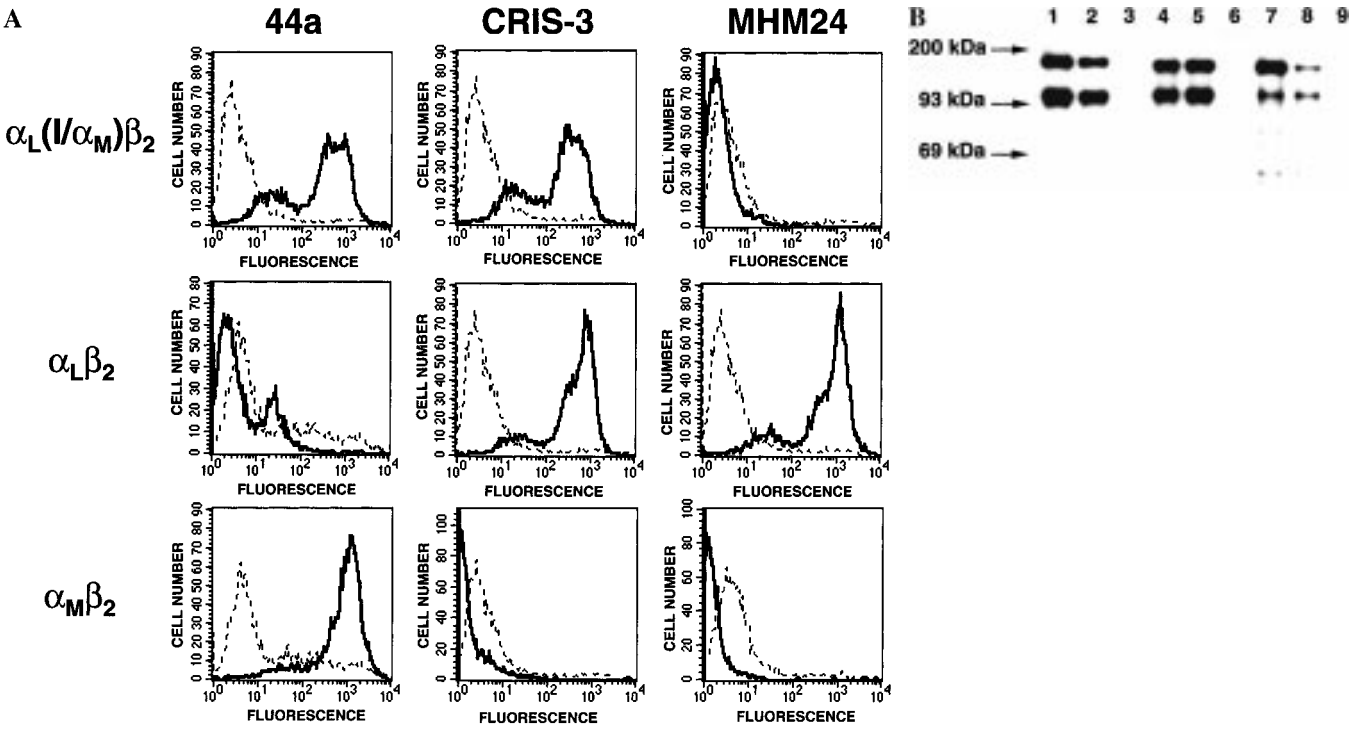

FIGURE 1: Chimeric $\alpha_L(I/\alpha_M)\beta_2$ receptor is expressed on the cell surface as a heterodimer. (A) FCAS analysis: $\alpha_M\beta_2$- or $\alpha_L\beta_2$-expressing 293 cells (10^6) were incubated with 5 μg of 44a, a mAb to the α_MI domain, CRIS-3, a mAb to a region outside the α_LI domain, MHM24, a mAb to the α_LI domain (solid lines), or an isotype matched control (dotted line) at 4 °C for 30 min. After three washes with PBS, the cells were stained with FITC-goat anti-mouse IgG and analyzed using FACScan, counting 10 000 events. (B) Surface labeling and immunoprecipitation. $\alpha_L\beta_2$- or $\alpha_M\beta_2$-expressing cells (1×10^6) were surface-labeled with biotin and immunoprecipitated with 10 μg of either 44a (lanes 1 and 4), TS1/22, a mAb to the α_LI domain (lane 7), IB4, a mAb to β_2 (lanes 2, 5, and 8), or IV.3, an irrelevant mAb (lanes 3, 6, and 9) overnight at 4 °C. After washing, the immunoprecipitates were subjected to SDS−PAGE (7% gels under nonreducing conditions), transferred to PVDF membrane, and immunoblotted with avidin−horseradish peroxidase conjugate. The membrane was then incubated with ECL substrate and exposed to Hyperfilm (Amersham, Buckinghamshire, England) for 1 min. Lanes: 1−3, $\alpha_M\beta_2$; 4−6, $\alpha_L(I/\alpha_M)\beta_2$; 7−9, $\alpha_L\beta_2$.

30 min, washed with PBS, and then resuspended in 500 μL of PBS. The FACS analysis was then performed using FACScan (Becton-Dickinson), counting 10 000 events. Mean fluorescence intensities were quantitated using the FACScan Program, and the values were used to compare $\alpha_M\beta_2$ expression levels and reactivity of the cells with various mAbs.

RESULTS

A Chimeric $\alpha_L\beta_2$ Receptor, $\alpha_L(I/\alpha_M)\beta_2$, Is Capable of Binding C3bi. Although $\alpha_M\beta_2$ and $\alpha_L\beta_2$ share the same β subunit and have structurally similar I domains, $\alpha_M\beta_2$ binds C3bi and $\alpha_L\beta_2$ does not (*3*). To test the contribution of the α_MI domain, as well as other regions of α_M to C3bi binding, the α_LI domain within the $\alpha_L\beta_2$ receptor was replaced with the α_MI domain. Previous attempts to construct *swap* mutants between $\alpha_M\beta_2$ and $\alpha_L\beta_2$ in COS cells were unsuccessful (*13*); but, using 293 cells, the chimeric receptor, $\alpha_L(I/\alpha_M)\beta_2$, was expressed on the cell surface. Efficient cell-surface expression of the chimeric receptor with appropriate characteristics is demonstrated by FACS analysis shown in Figure 1A. mAb 44a, which recognizes an epitope within the α_MI domain (see below), reacted with $\alpha_L(I/\alpha_M)\beta_2$ as did CRIS-3, which recognizes an α_L epitope outside of the α_LI domain (Figure 1A). Also, as expected, mAb MHM24, which recognizes the α_LI domain (*25*), failed to react with the chimeric receptor although it stained wild-type $\alpha_L\beta_2$ strongly. The presence of the α_MI domain within $\alpha_L\beta_2$ did not affect heterodimer formation: surface labeling and immunoprecipitation of $\alpha_L(I/\alpha_M)\beta_2$ with either mAbs 44a or TS1/22 against α_L or IB4 against β_2 yielded two bands of approximately 170 and 95 kDa on SDS−PAGE (Figure 1B). Since cell-surface expression of the β_2 subunit requires its complexation with a partnering α subunit, the reactivity of the $\alpha_L(I/\alpha_M)\beta_2$-bearing cells with mAb IB4 (Figure 1B) provides further support for efficient surface expression of the chimera.

The reactivity of $\alpha_L(I/\alpha_M)\beta_2$ with C3bi was assessed. As shown in Figure 2, this chimeric receptor bound C3bi well, comparable to wild-type $\alpha_M\beta_2$. The specificity of this interaction was demonstrated by the failure of the mock transfected or wild-type $\alpha_L\beta_2$-bearing cells to rosette with EC3bi. Furthermore, NIF, a specific ligand for the α_MI domain (*26*, *27*) and a potent inhibitor of C3bi binding to $\alpha_M\beta_2$ (*27*), blocked the interaction of C3bi with the chimeric receptor. Binding of C3bi by this chimera remained cation-dependent, as addition of 1 mM EDTA completely abrogated the C3bi binding (data not shown). These results suggest that the I domain of $\alpha_M\beta_2$ is the principal ligand binding interface for C3bi within the α_M subunit. Regions of α_M outside I domain are either not required or not centrally involved in C3bi binding.

A Narrow Region of the α_MI Domain Binds C3bi. We previously have mapped the NIF binding pocket within $\alpha_M\beta_2$ using homologue-scanning mutagenesis (*20*, *21*). This strategy is predicated on the crystal structures of the I domains of α_M (*18*) and α_L (*28*) and entails systematic switches of

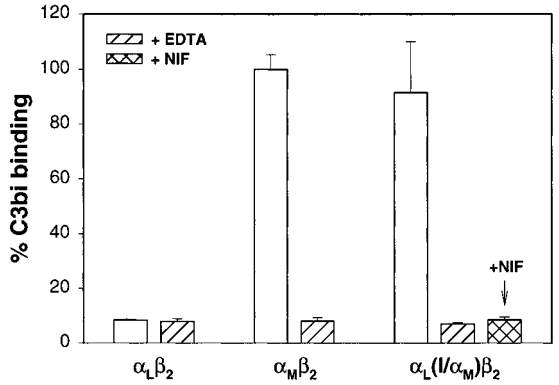

FIGURE 2: C3bi recognition by wild-type and chimeric $\alpha_L\beta_2$ transfectants. Biotinylated EC3bi (2×10^7) were added to 2×10^5 cells expressing $\alpha_M\beta_2$, $\alpha_L\beta_2$, or the $\alpha_L(I/\alpha_M)\beta_2$ chimera which had been preseeded onto polylysine-coated 24-well plates. After 60 min at 37 °C, the amount of bound EC3bi was determined using avidin−alkaline phosphatase and *p*-nitrophenyl phosphate, measuring the absorbance at 405 nm. The value for wild-type $\alpha_M\beta_2$ was taken as 100%. Specificity was demonstrated by addition of EDTA (1 mM) and NIF (5 μg/mL). Data are the means ± SD of 3−6 independent experiments.

homologous segments, α helices for α helices, β sheets for β sheets, and random coils for random coils, between α_M, which binds NIF, and α_L, which does not (*12*). We have shown that such homologous swapping does not alter the gross conformation of the resulting mutant $\alpha_M\beta_2$ receptors and that a total of 16 segment swaps within the I domains cover the outer hydrated surface of the α_MI domain (*21*). Since $\alpha_L\beta_2$ also does not interact with C3bi, these existing cell lines can be used to map the segments important for C3bi binding to the α_MI domain; this approach was implemented. As shown in Figure 3A, EC3bi rosetted well with wild-type $\alpha_M\beta_2$; approximately 60 EC3bi were bound to a typical $\alpha_M\beta_2$-expressing cell. Verifying the specificity of the interaction, C3bi binding was blocked by addition of NIF or EDTA. Most of the 16 mutants interacted with C3bi in a fashion comparable to the wild-type $\alpha_M\beta_2$ receptor. A few mutants, represented by $\alpha_M(E^{253}-R^{261})$ and $\alpha_M(K^{245}FG)$ in Figure 3A, lost their ability to bind the ligand. The C3bi binding activity of the 16 mutant $\alpha_M\beta_2$ receptors was quantitated using an avidin−biotin−alkaline phosphatase system and expressed as a percent of the activity of wild-type $\alpha_M\beta_2$-bearing cells (Figure 3B). The specificity of C3bi binding to each of the mutants which retained activity was verified by NIF and EDTA inhibition. The following mutants had similar (<1.5-fold different than wild-type $\alpha_M\beta_2$) C3bi binding activities: $\alpha_M(M^{153}-T^{159})$, $\alpha_M(E^{162}-L^{170})$, $\alpha_M(E^{178}-T^{185})$, $\alpha_M(Q^{190}-S^{197})$, $\alpha_M(K^{231}NAF)$, $\alpha_M(\Delta E^{262}G)$, $\alpha_M(D^{273}-K^{279})$, $\alpha_M(R^{281}-I^{287})$, $\alpha_M(F^{297}-T^{307})$, and $\alpha_M(Q^{309}-E^{314})$. The most dramatic losses of C3bi binding activities were restricted to six mutants: $\alpha_M(P^{147}-R^{152})$ (2.2-fold), $\alpha_M(P^{201}-G^{207})$ (5.6-fold), $\alpha_M(R^{208}-K^{217})$ (11.9-fold), $\alpha_M(K^{245}FG)$ (4.5-fold), $\alpha_M(\Delta D^{248}-Y^{252})$ (19.6-fold), and $\alpha_M(E^{253}-R^{261})$ (16.8-fold). These data suggest that the C3bi binding pocket is composed of these six segments. Similar expression levels for the wild-type receptor and the 16 mutants were verified by FACS analysis. With the six mutants showing defective C3bi binding, the mean fluorescence intensity obtained with mAb 44a did not vary by more than 1.5-fold compared to wild-type $\alpha_M\beta_2$-bearing cells. Thus, differences in receptor expression levels were not responsible for the loss of C3bi binding.

As shown in Figure 4, the six segments implicated in C3bi binding form a contiguous and narrow region supported by the underlying β strands. These segments surround the bound Mg^{2+} ion in the three-dimensional structure of the α_MI domain (*18*). The positioning of the cation within the C3bi binding pocket is consistent with the cation dependence of the C3bi−$\alpha_M\beta_2$ interaction.

Individual Amino Acids That Confer Binding Specificity for C3bi. Comparison of our previous delineation of the NIF binding pocket in the α_MI domain (*21*) with the location of the C3bi binding pocket in Figure 3b suggested one major difference between these two recognition sites: the $K^{245}FG$ sequence is required for C3bi but not for NIF binding. Specifically, mutation of the KFG sequence in α_M to the ATD sequence in α_L dramatically reduced C3bi binding (Figure 3b) but had no effect on NIF binding (*21*). To further characterize the basis for this specificity, additional mutagenesis experiments were conducted in which the K^{245} and F^{246} residues were altered. As shown in Figure 5, when residue K^{245} was mutated to Ala, C3bi binding activity was significantly reduced, whereas NIF binding was unaffected. In contrast, mutation of F^{246} to Ala had no effect on the capacity of the mutated $\alpha_M\beta_2$ to bind either C3bi or NIF (Figure 5). We also mutated K^{245} to Asp rather than to Ala to introduce a more dramatic change in this position. This mutation abolished both C3bi and NIF binding activities (Figure 5).

mAbs to $\alpha_M\beta_2$ Block C3bi Binding by Different Mechanisms. mAbs to $\alpha_M\beta_2$ can block C3bi binding by occupying portions of the ligand binding site or by inducing allosteric changes within the C3bi binding site. The homologue-scanning mutants were used to classify several $\alpha_M\beta_2$ mAbs with C3bi blocking functions (44, 44a, 904, and 2LPM19c). A representative FACS analysis for mutant $\alpha_M(E^{253}-R^{261})$ with three of these mAbs is shown in Figure 6A. While the mutant reacted well with mAbs 44a and 904, it failed to recognize mAb 44. Since mAb 44 reacts well with wild-type $\alpha_M\beta_2$, the $E^{253}-R^{261}$ segment is implicated as being part of the epitope for mAb 44. Similar FACS analyses were conducted with all 16 mutants for mAbs 44, 44a, and 904, and the results are summarized in Table 1. The epitope for mAb 44 maps to the segments $P^{201}-G^{207}$, $R^{208}-K^{217}$, $K^{245}FG$, $D^{248}-Y^{252}$, and $E^{253}-R^{261}$. These same five segments are involved in C3bi binding. Thus, the epitope for mAb 44 and the C3bi binding site overlap extensively. However, the recognition sites for C3bi and mAb 44 are not identical; C3bi binds to the segment $P^{147}-R^{152}$ (Figure 3B), whereas mAb 44 does not. The epitope for 44a mapped to segments $M^{153}-T^{159}$, $E^{162}-L^{170}$, and $Q^{309}-E^{314}$. This region partially overlaps with the region previously implicated in the binding of mAb 2LPM19c to $\alpha_M\beta_2$ (*29*), which resides at considerable distance from the C3bi binding pocket. Thus, like 2LPM19c, mAb 44a is likely to exert its effect on C3bi binding by perturbing the conformation of the α_M I domain. This conclusion is supported by a direct competition experiment (Figure 6B) where mAb 44a was shown to compete effectively with mAb 2LPM19c but had no effect on mAb 44 binding to $\alpha_M\beta_2$. Violette et al. (*30*) mapped the LM2/1 epitope to a specific peptide sequence, P^{291}PRDHVFQ. This recognition sequence is not included in our *homologue-*

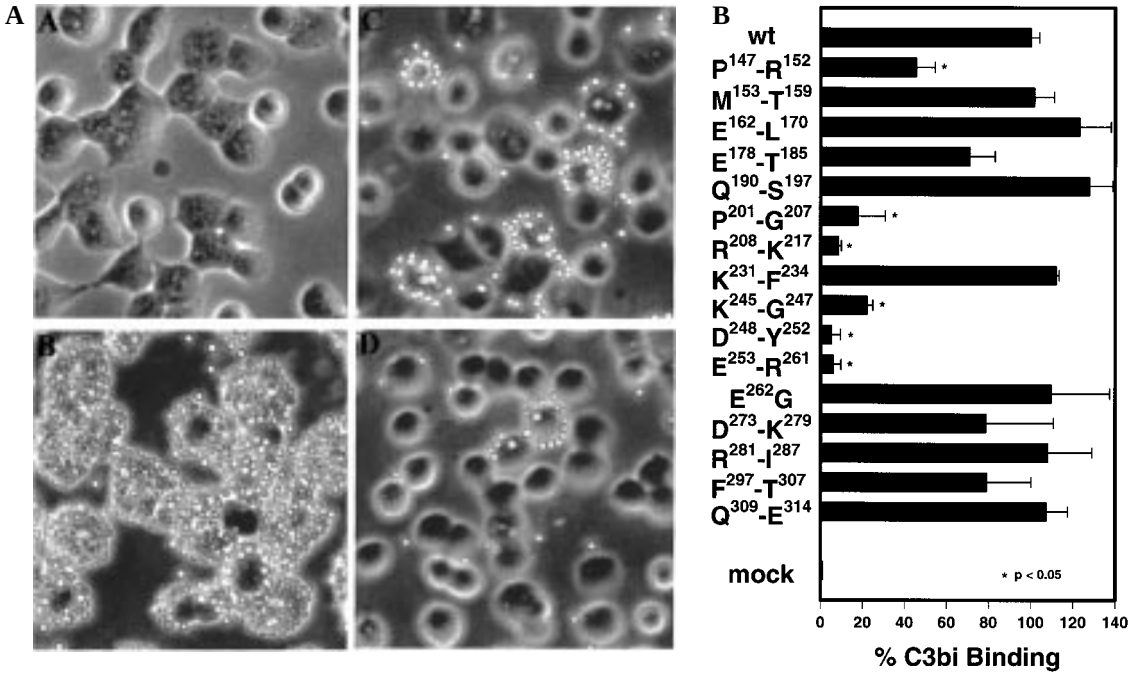

FIGURE 3: Interaction of wild-type and mutant $\alpha_M\beta_2$ receptors with C3bi. (A) EC3bi binding to wild-type or mutant $\alpha_M\beta_2$-expressing cells. Binding of EC3bi to $\alpha_M\beta_2$- or $\alpha_L\beta_2$-expressing cells was performed as described in Figure 2, and the cells were fixed with 1% paraformaldehyde and photographed: (A) $\alpha_L\beta_2$; (B) $\alpha_M\beta_2$; (C) $\alpha_M(K^{245}FG)\beta_2$; and (D) $\alpha_M(E^{253}-R^{261})\beta_2$. (B) C3bi binding activities of the homologue-scanning mutant $\alpha_M\beta_2$ receptors. Binding of biotinylated EC3bi to cells expressing mutant $\alpha_M\beta_2$ was performed as described in Figure 2.

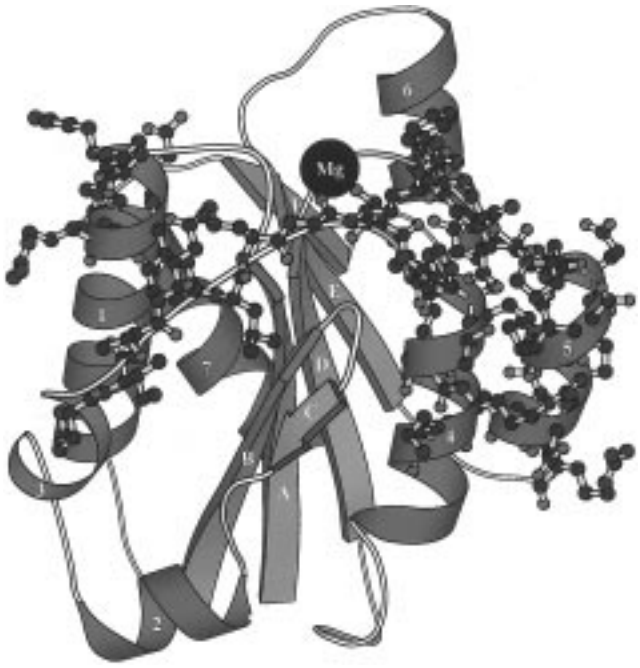

FIGURE 4: Molecular model of the C3bi binding pocket. The structure of α_MI domain is modeled from the crystal coordinates of α_MI domain (*18*) using the molscript software. The bound Mg^{2+} is shown in black. The numbers and letters refer to the helices and β strands, respectively, as assigned in the crystal structure of the α_MI domain. The C3bi binding pocket is depicted as balls and sticks.

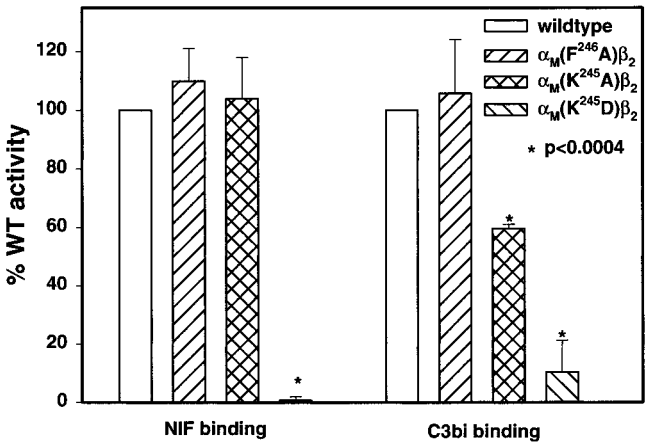

FIGURE 5: Comparison of the C3bi and NIF binding activities of $\alpha_M\beta_2$ containing single-point mutations. The value for wild-type $\alpha_M\beta_2$ was taken as 100%. For all mutants and the wild-type receptor, EC3bi binding can be blocked completely by addition of EDTA (1 mM). Data are the means ± SD of 3−6 independent experiments; *$p < 0.0004$ by Student *t*-test.

scanning mutants, and all 16 of our mutants reacted well with LM2/1. mAb 904 behaved very similarly to mAb LM2/1: it reacted well with all 16 mutants and with the $\alpha_L(I/\alpha_M)\beta_2$ chimera. The similarity in the reactivity patterns of these two mAbs, LM2/1 and 904, suggested that they may recognize a common or overlapping epitope. The FACS analyses shown in Figure 6C support this prediction. LM2/1 competed effectively with mAb 904 for binding to $\alpha_M\beta_2$, whereas a nonimmune control IgG had no effect.

DISCUSSION

Despite the importance of $\alpha_M\beta_2$−C3bi interaction in host defense, detailed information of the molecular basis for the specific recognition of C3bi by $\alpha_M\beta_2$ remains limited. In this study, we have mapped the C3bi binding site to a specific region of the α_MI domain and have identified a single amino acid residue which allows $\alpha_M\beta_2$ to distinguish C3bi from another cognate ligand, NIF. The three noncontiguous segments which compose the C3bi binding site are $P^{147}-R^{152}$, $P^{201}-K^{217}$, and $K^{245}-R^{261}$ within the α_MI domain. Among the residues within the C3bi binding pocket, K^{245} is

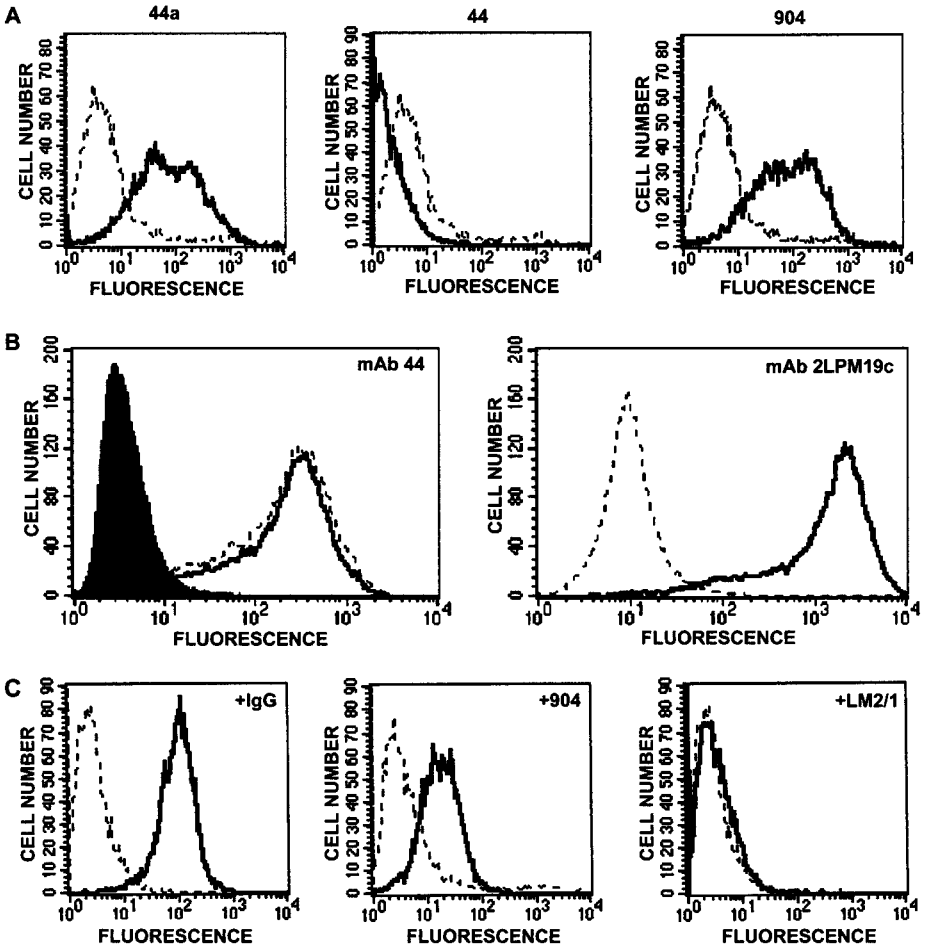

FIGURE 6: Epitope mapping of $\alpha_M\beta_2$ monoclonal antibodies. (A) mAb 44 recognizes the $E^{253}-R^{261}$ segment of the α_MI domain. $\alpha_M(E^{253}-R^{261})\beta_2$-expressing cells ($1 \times 10^6$) were stained with 5 μg of either mAb 44a, 44, or 904. FACS analysis was performed as described in Figure 1. (B) Blocking of mAb 2LPM19c, but not mAb 44, binding to $\alpha_M\beta_2$ by mAb 44a. $\alpha_M\beta_2$-expressing cells (1×10^6) were stained with either mAb 44-FITC or 2LPM19c-RPE in the presence of 5 μg of either mAb 44a (dashed line) or an irrelavent IgG (solid line). Bound mAb 2LPM19c or 44 was determined by FACS analysis. The background staining is shown here with mock-transfected cells (filled line). (C) Blocking of mAb 904 binding to $\alpha_M\beta_2$ by mAb LM2/1. $\alpha_M\beta_2$-expressing cells (1×10^6) were stained with biotinylated mAb 904 (solid line) or an irrelavent control IgG (dashed line). Bound antibodies were stained with FITC−avidin conjugate and analyzed by FACS. To compete with mAb 904 for binding to $\alpha_M\beta_2$, the cells were preincubated with 10 μg of either a control IgG, mAb 904, or LM2/1.

the critical residue which distinguishes the C3bi from the NIF binding sites in the receptor. The localization of C3bi binding pocket is supported by the observations that (1) when the α_MI domain is placed within the environment of the $\alpha_L\beta_2$ receptor, which does not interact with C3bi, the resultant chimeric receptor is capable of binding C3bi; (2) only the specified six-segment switches abrogated C3bi binding, but yet, as previously shown, switching these segments does not perturb the overall conformation of $\alpha_M\beta_2$ (*21*); (3) the epitope for a mAb which blocks the $\alpha_M\beta_2$−C3bi interaction maps to this same region.

At least three domains have been implicated in the ligand binding functions of the α_M subunit: the I domain, the EF-hand homologous region, and the lectin-like domain. While the role of the I domain in ligand binding is well-documented (*26*, *31*−*34*), the contributions of these other regions of α_M to C3bi recognition are still unclear. mAb OKM1, which recognizes an epitope in the EF-hand homologous region and the lectin-like domain, completely blocked Fg (*9*) and strongly inhibited C3bi binding to $\alpha_M\beta_2$ (*13*). Other mAbs which map to these regions of the receptor also are effective inhibitors of C3bi and ICAM-1 binding to $\alpha_M\beta_2$ (*13*). Furthermore, the EF-hand homologous regions in two other

Table 1: FACS Analysis Performed Using 5 μg of mAb and 10^6 Mutant $\alpha_M\beta_2$-Expressing Cells[a]

mutants	OKM1	LM2/1	2LPM19c	44	44a	904
wild-type	+	+	+	+	+	+
$\alpha_M(P^{147}-R^{152})$	+	+	+	+	+	+
$\alpha_M(M^{153}-T^{159})$	+	+	−	+	−	+
$\alpha_M(E^{162}-L^{170})$	+	+	−	+	−	+
$\alpha_M(E^{178}-T^{185})$	+	+	+	+	+	+
$\alpha_M(Q^{190}-S^{197})$	+	+	−	+	+	+
$\alpha_M(P^{201}-G^{207})$	+	+	+	−	+	+
$\alpha_M(R^{208}-K^{217})$	+	+	+	−	+	+
$\alpha_M(K^{231}NAF)$	+	+	+	+	+	+
$\alpha_M(K^{245}FG)$	+	+	+	−	+	+
$\alpha_M(\Delta D^{248}-Y^{252})$	+	+	+	−	+	+
$\alpha_M(E^{253}-R^{261})$	+	+	+	−	+	+
$\alpha_M(\Delta E^{262}G)$	+	+	+	+	+	+
$\alpha_M(D^{273}-K^{279})$	+	+	+	+	+	+
$\alpha_M(R^{281}-I^{287})$	+	+	+	+	+	+
$\alpha_M(F^{297}-T^{307})$	+	+	+	+	+	+
$\alpha_M(Q^{309}-E^{314})$	+	+	+	+	−	+
$\alpha_L(I/\alpha_M)\beta_2$	−	+	nd	+	+	+
$\alpha_L\beta_2$	−	−	−	−	−	−

[a] A "+" indicates that the mean fluoresence intensity of the mAb is at least 10 times that of the IgG control. A "−" indicates that the mean fluoresence intensity of the mAb is no more than that of the IgG control. nd, not determined.

integrins, $\alpha_L\beta_2$ and $\alpha_2\beta_1$, have been implicated in their ligand recognition (*35*, *36*). Nevertheless, it is not clear from these studies whether the EF-hand homologous region and the lectin-like domain are involved in direct ligand contact or play indirect modulatory roles in ligand recognition. Indeed, we have recently shown that the lectin-like domain modulates the binding function of the I domain for another $\alpha_M\beta_2$ ligand, *Candida albacans*, rather than directly contacting the ligand (*19*). In the present study, we constructed a chimeric receptor, $\alpha_L(I/\alpha_M)\beta_2$, in which the only component derived from $\alpha_M\beta_2$ is the I domain. This chimera was fully capable of binding C3bi (Figure 2), suggesting that the α_MI domain represents the principal C3bi contact surface within the α_M subunit. Therefore, regions outside I domain, such as the EF-hand region and the lectin-like domain, are not necessary for high-affinity C3bi recognition, or there is sufficient conservation of structure between these regions in α_L and α_M that they can be interchanged without affecting C3bi function. In either case, these other regions do no contribute to the selective recognition of C3bi by $\alpha_M\beta_2$.

The C3bi binding pocket identified in the α_MI domain with our homologue-scanning mutants overlaps extensively with the NIF binding pocket (*21*); five of the six segments implicated in C3bi binding also are involved in NIF binding. This overlap provides a molecular basis for the potent inhibition of C3bi binding by NIF. A single amino acid residue, K^{245}, is involved in the discrimination of C3bi and NIF by $\alpha_M\beta_2$. Mutation of this residue to Ala significantly reduced C3bi binding yet had no effect on NIF binding (Figure 5). This finding is consistent with an earlier report (*14*) that the N^{232}AFKILVVITDGEK peptide, which has K^{245} as its carboxy-terminus, is a potent inhibitor of C3bi binding to $\alpha_M\beta_2$. Since mutant $\alpha_M(K^{231}NAF)$ displays full C3bi binding activity (Figure 3B) and the remainder of the peptide sequence, KILVVITDGE, is conserved in α_M and α_L, the activity of the peptide must depend on preservation of its carboxy-terminal residue. Our results are also in agreement with the report of McGuire et al. (*22*), in which F^{246} and G^{247} were shown not to be important for C3bi binding. Finally, while our results emphasize the importance of K^{245} in C3bi binding, individual residues within the segments common to NIF and C3bi binding pockets may interact differentially with the two ligands.

Recently, it was reported that peptides derived from the complementarity determining regions (CDRs) of antibodies 44a and 904 have potent inhibitory effects on the function of $\alpha_M\beta_2$ (*37*). $\alpha_M\beta_2$-dependent neutrophil activation plays a central role in the pathogenesis of many diseases including sepsis, respiratory distress syndrome, and ischemia−reperfusion injuries (*38*); antibodies against $\alpha_M\beta_2$ have been shown effective in prevention of tissue injuries in various disease models (*39*−*43*). Therefore, peptides from the CDRs of function-blocking mAbs could provide lead structures for the development of potential $\alpha_M\beta_2$ antagonists (*37*). Accordingly, we have used our panel of mutant receptors to determine how several function-blocking mAbs exert their activity on $\alpha_M\beta_2$. Although Violette et al. previously had located the recognition sites of mAbs 44, 904, 2LPM19c, and LM2/1 to the α_MI domain (*30*), they had not conducted high-resolution epitope mapping. We have shown that mAb 44 recognizes the same segments (P^{201}−K^{217}, and K^{245}−R^{261}) as C3bi (Table 1). The fact that this mAb blocks C3bi

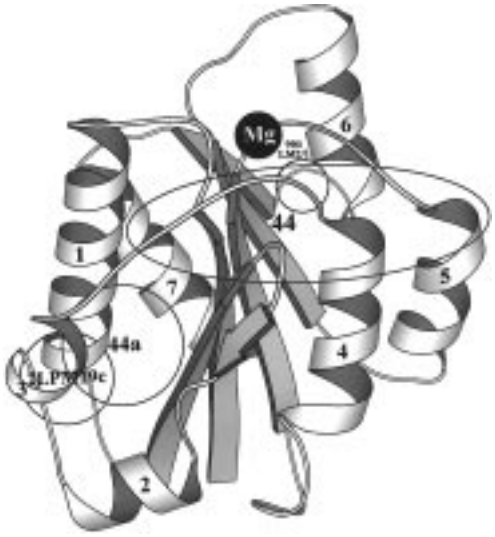

FIGURE 7: Epitopes for $\alpha_M\beta_2$ blocking antibodies. The epitope for each mAb is indicated by a circle superimposed on the molecular model of the α_MI domain (see Figure 4). The bound Mg^{2+} is shown in black. The epitopes for mAbs LM2/1 and 904 are located near the end of helix 6, which is quite distant from the mAb 44 epitope.

recognition (*11*, *44*) provides additional support for the involvement of these regions in C3bi binding. Surprisingly, another blocking mAb, 44a, recognizes a distinct region (M^{153}−T^{159}, E^{162}−L^{170}, and Q^{309}−E^{314}) far from the C3bi binding site. This mAb has an epitope which overlaps that of mAb 2LPM19c, which we have previously shown to be an allosteric inhibitor of $\alpha_M\beta_2$ ligand binding (*29*). Thus, it is likely that mAb 44a inhibits C3bi binding through induction of conformational changes which perturb the binding function of the receptor, and the peptide derived from CDR of mAb 44a might exert its inhibitory function in an allosteric manner. Consistent with this hypothesis, there is no homology between the inhibitory peptide derived from mAb 44a and one of the $\alpha_M\beta_2$ ligands, ICAM-1 (*37*). The localization of the epitopes for mAbs LM2/1 and 904 was based on these following experiments. First, both mAbs reacted well with all 16 mutants and the $\alpha_L(I/\alpha_M)\beta_2$ chimeric receptor, but not with $\alpha_L\beta_2$, suggesting that their epitopes should reside within the α_MI domain but in regions not covered by our homologue-scanning mutants. Second, the epitope for LM2/1 previously had been located by Violette et al. (*30*) to the sequence P^{291}PRDHVFQ, which lies in the loop region between helix 6 and β sheet F and is not covered by our mutants (Figure 7). Third, mAb LM2/1 was found to effectively compete with mAb 904 for binding to $\alpha_M\beta_2$, but mAb 904 does not recognize the above peptide (*30*), suggesting that the epitopes for mAbs 904 and LM2/1 overlap but are not identical. The epitopes for both mAbs are distant from the C3bi binding site, which is in agreement with the fact that both mAbs are poor inhibitors of C3bi binding to the receptor (*13*, *44*).

In summary, we have mapped the binding pocket for C3bi in $\alpha_M\beta_2$. The specificity of $\alpha_M\beta_2$ for C3bi is critically dependent upon residue K^{245}. Though both mAbs 44 and 44a are potent inhibitors of C3bi binding to $\alpha_M\beta_2$, they exert this effect by different mechanisms. The former blocks $\alpha_M\beta_2$ function by direct competition for the ligand binding site, whereas the latter induces a conformational change which perturbs the ligand binding pocket. In addition, we show that

the I domain of $\alpha_M\beta_2$ is the principal contact interface for C3bi. Regions outside I domain are not required for selective binding of C3bi to $\alpha_M\beta_2$. Using our homologue-scanning mutants, we have mapped the C3bi binding site to a narrow region composed of segments $P^{147}-R^{152}$, $P^{201}-K^{217}$, and $K^{245}-R^{261}$. This binding site contains the entire NIF binding pocket, plus an additional residue, K^{245}, that is not required for NIF binding. The cation binding site within the α_MI domain is located within the C3bi segment and may participate directly in ligand binding. Since phagocytosis of opsonized foreign pathogens represents a primary host defense mechanism and the importance of $\alpha_M\beta_2$ in phagocytosis has been well-established from studies using mAbs and $\alpha_M\beta_2$-deficient mice (*6*, *45*), knowledge of the C3bi binding site within $\alpha_M\beta_2$ will help us understand how this receptor contributes to leukocyte functions. Identification of the epitopes of $\alpha_M\beta_2$-blocking mAbs will also help us in the design of mAb-based therapeutic agents.

ACKNOWLEDGMENT

The authors wish to thank Yin Chen for her excellent technical assistance. FACS analyses were conducted in a facility established with a gift from the WM Keck Foundation.

NOTE ADDED IN PROOF

While this manuscript was in preparation, several individual residues within the segments identified in this paper were reported to be critical for $\alpha_M\beta_2$−C3bi interaction [Li, R., Rieu, P., Griffith, D. L., Scott, D., and Arnaout, M. A. *J. Cell. Biol. 143*, 1523−1534].

REFERENCES

1. Anderson, D. C., Miller, L. J., Schmalsteig, F. C., Rothlein, R., and Springer, T. A. (1986) *J. Immunol. 137*, 15−27.
2. Springer, T. A. (1990) *Nature 346*, 425−434.
3. Arnaout, M. A. (1990) *Blood 75*, 1037−1050.
4. Smith, C. W., Marlin, S. D., Rothlein, R., Toman, C., and Anderson, D. C. (1989) *J. Clin. Invest. 83*, 2008−2017.
5. Shappell, S. B., Toman, C., Anderson, D. C., Taylor, A. A., Entman, M. L., and Smith, C. W. (1990) *J. Immunol. 144*, 2702−2711.
6. Coxon, A., Rieu, P., Barkalow, F. J., Askari, S., Sharpe, A. H., Von Andrian, U. H., Arnaout, M. A., and Mayadas, T. N. (1996) *Immunity 5*, 653−666.
7. Schmalstieg, F. C. (1988) *Pediatr. Infect. Dis. J. 867*, 872.
8. von Asmuth, E. J., van der Linden, C. J., Leeuwenberg, J. F., and Buurman, W. A. (1991) *J. Immunol. 147*, 3869−3875.
9. Altieri, D. C., Bader, R., Mannucci, P. M., and Edgington, T. S. (1988) *J. Cell Biol. 107*, 1893−1900.
10. Diamond, M. S., Staunton, D. E., de Fougerolles, A. R., Stacker, S. A., Garcia-Aguilar, J., Hibbs, M. L., and Springer, T. A. (1990) *J. Cell Biol. 111*, 3129−3139.
11. Beller, D. E., Springer, T. A., and Schreiber, R. D. (1982) *J. Exp. Med. 156*, 1000−1010.
12. Moyle, M., Foster, D. L., McGrath, D. E., Brown, S. M., Laroche, Y., De Meutter, J., Bogowitz, C. A., Fried, V. A., Ely, J. A., and et al. (1994) *J. Biol. Chem. 269*, 10008−10015.
13. Diamond, M. S., Garcia-Aguilar, J., Bickford, J. K., Corbí, A. L., and Springer, T. A. (1993) *J. Cell Biol. 120*, 1031−1043.
14. Ueda, T., Rieu, P., Brayer, J., and Arnaout, M. A. (1994) *Proc. Natl. Acad. Sci. U.S.A. 91*, 10680−10684.
15. Zhang, L., and Plow, E. F. (1996) *J. Biol. Chem. 271*, 18211−18216.
16. Bajt, M. L., Goodman, T., and McGuire, S. L. (1995) *J. Biol. Chem. 270*, 94−98.
17. Michishita, M., Videm, V., and Arnaout, M. A. (1993) *Cell 72*, 857−867.
18. Lee, J.-O., Rieu, P., Arnaout, M. A., and Liddington, R. (1995) *Cell 80*, 631−638.
19. Forsyth, C. B., Plow, E. F., and Zhang, L. (1998) *J. Immunol. 161*, 6198−6205.
20. Cunningham, B. C., Jhurani, P., Ng, P., and Wells, J. A. (1989) *Science 243*, 1330−1336.
21. Zhang, L., and Plow, E. F. (1997) *J. Biol. Chem. 272*, 17558−17564.
22. McGuire, S. L., and Bajt, M. L. (1995) *J. Biol. Chem. 270*, 25866−25871.
23. Zhang, L., and Castellino, F. J. (1990) *Biochemistry 29*, 10828−10834.
24. Bilsland, C. A., Diamond, M. S., and Springer, T. A. (1994) *J. Immunol. 152*, 4582−4589.
25. Champe, M., McIntyre, B. W., and Berman, P. W. (1995) *J. Biol. Chem. 270*, 1388−1394.
26. Muchowski, P. J., Zhang, L., Chang, E. R., Soule, H. R., Plow, E. F., and Moyle, M. (1994) *J. Biol. Chem. 269*, 26419−26423.
27. Rieu, P., Ueda, T., Haruta, I., Sharma, C. P., and Arnaout, M. A. (1994) *J. Cell Biol. 127*, 2081−2091.
28. Qu, A., and Leahy, D. J. (1995) *Proc. Natl. Acad. Sci. U.S.A. 92*, 10277−10281.
29. Zhang, L., and Plow, E. F. (1996) *J. Biol. Chem. 271*, 29953−29957.
30. Violette, S. M., Rusche, J. R., Purdy, S. R., Boyd, J. G., Cos, J., and Silver, S. (1995) *J. Immunol. 155*, 3092−3101.
31. Zhou, L., Lee, D. H., Plescia, J., Lau, C. Y., and Altieri, D. C. (1994) *J. Biol. Chem. 269*, 17075−17079.
32. Kamata, T., and Takada, Y. (1994) *J. Biol. Chem. 269*, 26006−26010.
33. Randi, A. M., and Hogg, N. (1994) *J. Biol. Chem. 269*, 12395−12398.
34. Calderwood, D. A., Tuckewell, D. S., Eble, J., Kuhn, K., and Humphries, M. J. (1997) *J. Biol. Chem. 272*, 12311−12317.
35. Stanley, P., Bates, P. A., Harvey, J., Bennett, R. I., and Hogg, N. (1994) *EMBO J. 13*, 1790−1798.
36. Dickeson, S. K., Walsh, J. J., and Santoro, S. A. (1997) *J. Biol. Chem. 272*, 7661−7668.
37. Feng, Y., Chung, D., Garrard, L., McEnroe, G., Lim, D., Scardina, J., McFadden, K., Guzzetta, A., Lam, A., Abraham, J., Liu, D., and Endemann, G. (1998) *J. Biol. Chem. 273*, 5625−5630.
38. Albelda, S. M., Smith, C. W., and Ward, P. A. (1994) *FASEB J. 8*, 504−512.
39. Chopp, M., Zhang, R. L., Chen, H., Li, Y., Jiang, N., and Rusche, J. R. (1994) *Stroke 25*, 869−875.
40. Simpson, P. J., Todd, R. F., III, Fantone, J. C., Mickelson, J. K., Griffin, J. D., Lucchesi, B. R., Adams, M. E., Hoff, P., and Rogers, C. E. (1988) *J. Clin. Invest. 81*, 624−629.
41. Nolte, D., Hecht, R., Schmid, P., Botzlar, A., Menger, M. D., Neumueller, C., Sinowatz, F., Vestweber, D., and Messmer, K. (1994) *Am. J. Physiol. Heart Circ. Physiol. 267*, H1320−H1328.
42. Minamino, T., Kitakaze, M., Node, K., Funaya, H., Inoue, M., Hori, M., and Kamada, T. (1996) *J. Mol. Cell. Cardiol. 28*, 1575−1581.
43. Jaeschke, H., Farhood, A., Bautista, A. P., Spolarics, Z., Spitzer, J. J., and Smith, C. W. (1993) *Hepatology 17*, 915−923.
44. Dana, N., Styrt, B., Griffin, J. D., Todd, R. F., III, Klempner, M. S., and Arnaout, M. A. (1986) *J. Immunol. 137*, 3259−3263.
45. Lu, H., Smith, C. W., Perrard, J., Bullard, D., Tang, L., Entman, M. L., Beaudet, A. L., and Ballantyne, C. M. (1997) *J. Clin. Invest. 99*, 1340−1350.

BI990141H